

**Layered ferromagnet-superconductor structures: The  $\pi$  state and proximity effects**

Klaus Halterman\*

*Sensor and Signal Sciences Division, Naval Air Warfare Center, China Lake, California 93555, USA*Oriol T. Valls<sup>†</sup>*School of Physics and Astronomy and Minnesota Supercomputer Institute, Minneapolis, Minnesota 55455, USA*

(Received 23 June 2003; published 30 January 2004)

We investigate clean multilayered structures of the *SFS* and *SF<sub>2</sub>FS* type (where the *S* layer is intrinsically superconducting and the *F* layer is ferromagnetic), at low temperature, through numerical solution of the self-consistent Bogoliubov–de Gennes equations for these systems. We obtain results for the pair amplitude, the local density of states, and the local magnetic moment. We find that as a function of the thickness  $d_F$  of the magnetic layers separating adjacent superconductors, the ground state energy varies periodically between two stable states. The first state is an ordinary “0 state,” in which the order parameter has a phase difference of zero between consecutive *S* layers, and the second is a “ $\pi$  state,” where the sign alternates, corresponding to a phase difference of  $\pi$  between adjacent *S* layers. This behavior can be understood from simple arguments. The density of states and the local magnetic moment also reflect this periodicity.

DOI: 10.1103/PhysRevB.69.014517

PACS number(s): 74.50.+r, 74.25.Fy

**I. INTRODUCTION**

The study of layered ferromagnet-superconductor (*F/S*) heterostructure has sustained the active interest of many researchers. This is due in great part to continuing and recent progress in the preparation and fabrication of multilayer systems, and to the potential use of such heterostructures in various important applications. In particular, structures consisting of alternating ferromagnet (*F*) and superconductor (*S*) layers may exhibit, in certain cases, a ground state in which the difference  $\Delta\phi$  between the order parameter phase of adjacent superconductor layers equals  $\pi$ . These are the so called “ $\pi$  junctions.” These *F/S* hybrid structures offer advances in the field of nanoscale technology, including quantum computing,<sup>1</sup> where the implementation of a quantum two-level system is based on superconducting loops of  $\pi$  junctions. Furthermore, artificial composites involving a superconductor sandwiched between two ferromagnets, the design of which follows from giant magnetoresistive (GMR) devices, show potential use as spin valves<sup>2–4</sup> and nonvolatile memory elements.<sup>5</sup> An essential principle behind many of these spin-based devices is the damped oscillatory nature of the Cooper pairs in the ferromagnet region and the associated phase shift in the superconducting order parameter.

The coupling between nearby superconductors separated by a ferromagnet is a property that follows from the proximity effects, which in the context of *F/S* multilayers consist of the existence of superconducting correlations in the ferromagnet and magnetic correlations in the superconductor, arising from their mutual influence. The resulting superconducting phase coherence is quantified by the pair amplitude  $F(\mathbf{r}) = \langle \hat{\psi}_\downarrow(\mathbf{r}) \hat{\psi}_\uparrow(\mathbf{r}) \rangle$ , where the  $\hat{\psi}_\sigma$  are the usual annihilation operators. It is now well established that the leakage of superconductivity is due to the process of the Andreev reflection,<sup>6</sup> whereby a quasiparticle incident on a *F/S* interface is retroreflected as a quasihole of opposite spin. It is in turn the coherent superposition of these states, spin split by

the exchange field in the ferromagnet, that ultimately leads to damped oscillations of  $F(\mathbf{r})$  in the magnet, with a characteristic length  $\xi_F$  typically much smaller than the superconducting coherence length  $\xi_0$ . These oscillations are akin to high-field oscillatory phenomena described a long time ago.<sup>7,8</sup> In the absence of currents and magnetic fields, the modulation of the order parameter determines whether two neighboring superconductor layers share a stable  $\pi$  or 0 phase difference. For a multilayer *F/S* heterostructure with ferromagnet layers of order  $\pi\xi_F$  in width, it is intuitively evident, taking into account the continuity of  $F(\mathbf{r})$  across the *F/S* interface and the particular oscillatory nature of the pair amplitude in the ferromagnet, that a configuration will result in which it is energetically favorable to have a phase difference of  $\Delta\phi = \pi$ , rather than zero, between successive superconducting layers. This indeed turns out to be the case.

Although recently there has been a surge of interest in the study of *F/S* multilayer structures (see, e.g., the theoretical work of Refs. 9–28 and the experimental work discussed below), work on superconductor-ferromagnet-superconductor (*SFS*) Josephson junctions started long ago.<sup>29</sup> The Josephson current was calculated for a short weak link in the clean limit, and found to exhibit oscillations as a function of the ferromagnet exchange field.<sup>30</sup> It was later demonstrated that for a *SFS* sandwich obeying the dirty limit conditions, the critical current oscillates as a function of the thickness of the magnet and of the exchange field.<sup>15</sup> A more detailed analysis of dirty  $\pi$  junctions near the critical temperature allowed for differing transparencies of the ferromagnet-superconductor interfaces.<sup>16</sup> Many interesting phenomena have been proposed or discussed. Calculations were more recently performed for a *SFS* junction with arbitrary impurity concentration. For nonhomogeneous magnetization,<sup>18,26</sup> the superconductor may exhibit a nonzero triplet component extending well into the magnet. For quasi-two-dimensional, tight-binding, *F/S* atomic-scale multilayers, the ground state was shown in some cases to be the  $\pi$  state,<sup>19</sup> and the density of states (DOS) exhibited prominent features that depend

critically on the exchange field and transfer integral parameters.<sup>20</sup> For multilayer structures consisting of two ferromagnets and an insulator sandwiched between two superconductors, an enhancement of the Josephson current was predicted<sup>21,22</sup> for antiparallel alignment of the magnetization in the ferromagnet layers. Spin-orbit scattering<sup>17,23</sup> and changing the relative orientation angle of the in-plane magnetizations<sup>24</sup> were shown to significantly modify the behavior of the dc Josephson current.

The rapidly evolving theoretical views compounded with technological advances that permit the fabrication of well-characterized heterostructures has prompted a considerable number of experimental investigations of  $\pi$  coupling on several fronts. A study of the superconducting transition temperature for  $F/S$  multilayers revealed oscillatory behavior as a function of ferromagnet thickness.<sup>31</sup> For  $\pi$  junctions involving relatively weak ferromagnets, variations in temperature can induce a crossover from  $\Delta\phi=0$  to the  $\pi$  state, and this was observed<sup>32</sup> as oscillations of the critical current versus temperature. The transition to the  $\pi$  state is also reflected in critical current measurements for Josephson junctions in which the ferromagnet layer separating the two superconductors was systematically varied.<sup>33</sup> The superconducting phase was measured directly<sup>34</sup> using SQUID's made of  $\pi$  junctions, demonstrating a half quantum flux shift in the diffraction pattern. Direct evidence of the oscillatory behavior of the superconducting correlations in the ferromagnet was found through tunneling spectroscopy measurements that yielded inversions in the DOS for a thin ferromagnetic film, in contrast with the behavior in a superconductor.<sup>35</sup>

A common feature that pervades most of the theoretical work mentioned above is the use of quasiclassical formalisms, often compounded by the neglect of self-consistency for the space-dependent pair potential,  $\Delta(\mathbf{r})$ . These approximations do have the advantage of providing an accessible and efficient method to approximately calculate properties of inhomogeneous superconducting systems, while avoiding the cumbersome numerical issues that arise when attempting to solve the corresponding, much more complicated, self-consistent microscopic equations. The general underlying drawback of such approximations, however, is the elimination from consideration of phenomena at the atomic length scale given by the Fermi wavelength,  $\lambda_F$ , as can be seen in the derivation of the Eilenberger equations.<sup>36</sup> Further approximations follow when the assumption is made that the mean free path is much shorter than  $\xi_0$ , in which case the Eilenberger equations reduce to the widely used Usadel equations.<sup>37</sup> The elimination of the relatively small length scales poses problems for quasiclassical methods (even when self-consistent) when interfacial scattering is involved,<sup>17</sup> or when the geometry or potentials have sharp variations on the atomic scale. These issues, of increasing experimental importance given the ever-improving quality of the experimental samples, often require nontrivial effective boundary conditions that must supplement the basic equations. The problem worsens when dealing with multilayer structures, where the successive reflections and transmission of quasiparticles creates closed trajectories<sup>38</sup> that may render the quasiclassical approximation scheme inapplicable.

In this paper we investigate the proximity effect and associated electronic properties of clean three-dimensional  $F/S$  multilayer structures comprised of alternating superconductor and ferromagnet layers. Our emphasis is on the study of the existence of pair potential behavior of the  $\pi$  type. We implement a complete self-consistent microscopic theory that treats all the characteristic length scales on an equal footing, and thus can accommodate all quantum interference effects that are likely to be pertinent. The problem will be solved from a wave function approach using the Bogoliubov–de Gennes (BdG) equations. To do so, we extend an earlier method<sup>39</sup> used for a single  $F/S$  structure, to allow for a more complicated geometry, consisting of an arbitrary number of layers. Self-consistency is rigorously included, as it has been demonstrated<sup>39,40</sup> that this is essential in the study of the proximity effect at  $F/S$  interfaces.

We present in Sec. II the geometry and the numerical approach we take to solve the microscopic BdG equations and obtain the self-consistent energy spectra (eigenvalues and eigenfunctions). We also explain in some detail how the local DOS and the ground state energy are calculated. In Sec. III we first present our results for  $SFS$  structures and show examples of the relevant quantities: these include first of all the pair amplitude, which is used to illustrate the cases in which either the 0 or  $\pi$  state is energetically favored. The thickness of the  $F$  layer or layers turns out to be the decisive parameter, with the zero and  $\pi$  states periodically alternating in stability as this quantity varies. The experimentally accessible DOS averaged over a superconducting layer is next discussed: results for both the sum and the difference of the up and down spin terms are presented and their correlation with the zero or  $\pi$  states demonstrated. Results for the local magnetic moment, which we show how to calculate from the spin-dependent local DOS, are also given: in the superconductor this quantity measures the penetration of magnetic correlations. We analyze also, in a similar fashion, a more complicated five-layer structure, discuss the similarities and differences between the two geometries, and the generalization of our results to more complicated structures. Finally in Sec. IV we briefly summarize our results and discuss potential experimental implications and future work.

## II. METHOD

In this paper we consider a semi-infinite multilayer structure of total length  $d$  in the  $z$  direction, consisting of an odd number  $N_L$  of alternate superconductor ( $S$ ) and ferromagnetic ( $F$ ) layers, each of width  $d_S$  and  $d_F$ , respectively (see Fig. 1). The sandwich configuration is such that the complete structure begins and ends with a superconductor layer. The free surfaces at  $z=0$  and  $z=d$  are specularly reflecting. The basic methodology we use is an extension of that which has been previously discussed.<sup>39,40</sup> Upon taking into account the translational invariance in the  $x-y$  plane, one can immediately write the BdG equations<sup>41</sup> for the spin-up and spin-down quasiparticle and quasihole wave functions ( $u_n^\uparrow, v_n^\downarrow$ ),

$$\begin{bmatrix} \mathcal{H} - h_0(z) & \Delta(z) \\ \Delta(z) & -[\mathcal{H} + h_0(z)] \end{bmatrix} \begin{bmatrix} u_n^\uparrow(z) \\ v_n^\downarrow(z) \end{bmatrix} = \epsilon_n \begin{bmatrix} u_n^\uparrow(z) \\ v_n^\downarrow(z) \end{bmatrix}, \quad (1)$$

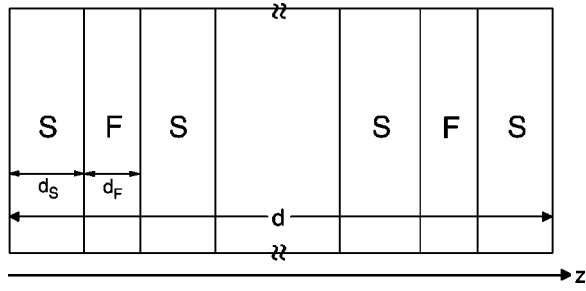


FIG. 1. Schematic of the model geometry used in this paper. The total thickness in the  $z$  direction is  $d$ , and the thicknesses of the  $S$  and  $F$  layers are  $d_S$  and  $d_F$  as indicated. There is a total number  $N_L$  of layers  $N_L=3$  and  $N_L=5$  in this work, with the outer ones being superconducting.

where the free-particle Hamiltonian is defined as,

$$\mathcal{H} \equiv -\frac{1}{2m} \frac{\partial^2}{\partial z^2} + \varepsilon_{\perp} - E_F(z). \quad (2)$$

Here  $\varepsilon_{\perp}$  is the transverse kinetic energy, the  $\epsilon_n$  are the quasiparticle energy eigenvalues, and  $\Delta(z)$  is the pair potential, described below. The magnetic exchange energy  $h_0(z)$  is equal to a constant  $h_0$  in the ferromagnet layers, and zero elsewhere. A potential  $U(z)$  describing interface scattering can easily be added to Eq. (2). We define the quantity  $E_F(z)$  to equal  $E_{FM}$  in the magnetic layers, so that in these regions,  $E_{F\uparrow} = E_{FM} + h_0$  and  $E_{F\downarrow} = E_{FM} - h_0$ . Likewise, in the superconducting layers,  $E_F(z) = E_{FS}$ . The dimensionless parameter  $I \equiv h_0/E_{FM}$  characterizes the strength of the magnet. At  $I=1$ , one therefore reaches the half metallic limit. From the symmetry of the problem, the solutions for the other set of wave functions ( $u_n^{\downarrow}, v_n^{\downarrow}$ ) are easily obtained from those of Eqs. (1) by allowing for both positive and negative energies. The BdG equations are completed by the self-consistency condition for the pair potential,

$$\Delta(z) = \frac{g(z)}{2} \sum_{\epsilon_n \leq \omega_D} [u_n^{\uparrow}(z)v_n^{\downarrow}(z) + u_n^{\downarrow}(z)v_n^{\uparrow}(z)] \tanh(\epsilon_n/2T), \quad (3)$$

where  $T$  is the temperature,  $g(z)$  is the effective coupling describing the electron-electron interaction, which we take to be a constant  $g$  within the superconductor layers and zero within the ferromagnet layers, and  $\omega_D$  is the Debye energy. We have not included spin-orbit coupling, and assumed that all of the  $F$  layers are magnetically aligned and hence<sup>26</sup> considered singlet pairing only in the  $s$  wave.

We solve<sup>40</sup> Eq. (1) by expanding the quasiparticle amplitudes in terms of a set of orthonormal basis vectors,  $u_n^{\uparrow}(z) = \sum_q u_{nq}^{\uparrow} \phi_q(z)$  and  $v_n^{\downarrow}(z) = \sum_q v_{nq}^{\downarrow} \phi_q(z)$ . We use the complete set of eigenfunctions  $\phi_q(z) = \langle z|q\rangle = \sqrt{2/d} \sin(k_q z)$ , where  $k_q = q/\pi d$ , and  $q$  is a positive integer. The finite range of the pairing interaction  $\omega_D$  permits the number  $N$  of such basis vectors to be cut off in the usual way.<sup>39</sup> Once this is done, we arrive at the following  $2N \times 2N$  matrix eigensystem,

$$\begin{bmatrix} H^+ & D \\ D & H^- \end{bmatrix} \Psi_n = \epsilon_n \Psi_n, \quad (4)$$

where  $\Psi_n^T = (u_{n1}^{\uparrow}, \dots, u_{nN}^{\uparrow}, v_{n1}^{\downarrow}, \dots, v_{nN}^{\downarrow})$ . The matrix elements  $H_{qq'}^{\pm}$ , connecting  $\phi_q$  to  $\phi_{q'}$ , are constructed from the real-space quantities in Eq. (1),

$$\begin{aligned} H_{qq'}^+ &= \langle q | \left[ -\frac{1}{2m} \frac{\partial^2}{\partial z^2} + \varepsilon_{\perp} - E_F(z) \right] - h_0(z) | q' \rangle \\ &= \left[ \frac{k_q^2}{2m} + \varepsilon_{\perp} \right] \delta_{qq'} - \int_0^d dz \phi_q(z) E_{F\uparrow}(z) \phi_{q'}(z) \\ &\quad - \int_0^d dz \phi_q(z) E_F(z) \phi_{q'}(z). \end{aligned} \quad (5a)$$

The expression for  $H_{qq'}^-$  is calculated similarly. The off-diagonal matrix elements  $D_{qq'}$  are given as

$$D_{qq'} = \langle q | \Delta(z) | q' \rangle = \int_0^d dz \phi_q(z) \Delta(z) \phi_{q'}(z). \quad (5b)$$

After performing the integrations, Eq. (5a) can be expressed as

$$\begin{aligned} H_{qq'}^+ &= \sum_{n=1}^{(N_L+1)/2} \left\{ \frac{E_{F\uparrow}}{d} \left[ \frac{\sin\{(k_q - k_{q'})[n(d_F + d_S) - d_F]\}}{(k_q - k_{q'})} \right. \right. \\ &\quad - \frac{\sin[(k_q - k_{q'})(n-1)(d_F + d_S)]}{(k_q - k_{q'})} \\ &\quad + \frac{\sin[(k_q + k_{q'})(n-1)(d_F + d_S)]}{(k_q + k_{q'})} \\ &\quad \left. - \frac{\sin\{(k_q + k_{q'})[n(d_F + d_S) - d_F]\}}{(k_q + k_{q'})} \right] \\ &\quad - \frac{E_{FS}}{d} \left[ \frac{\sin(k_q - k_{q'})[n(d_F + d_S) - d_F]}{(k_q - k_{q'})} \right. \\ &\quad - \frac{\sin[(k_q - k_{q'})(n-1)(d_F + d_S)]}{(k_q - k_{q'})} \\ &\quad + \frac{\sin[(k_q + k_{q'})(n-1)(d_F + d_S)]}{(k_q + k_{q'})} \\ &\quad \left. \left. - \frac{\sin\{(k_q + k_{q'})[n(d_F + d_S) - d_F]\}}{(k_q + k_{q'})} \right] \right\}, \quad q \neq q'. \end{aligned} \quad (6a)$$

The diagonal matrix elements are somewhat simpler, and are written

$$\begin{aligned}
H_{qq}^+ = & \frac{k_q^2}{2m} + \varepsilon_{\perp} - \frac{E_{F\uparrow}}{2d} \left[ (N_L - 1)d_F \right. \\
& + \frac{1}{k_q} \sum_{n=1}^{(N_L+1)/2} \sin\{2k_q[n(d_F + d_S) - d_F]\} \\
& \left. - \sin[2k_q(n-1)(d_F + d_S)] \right] - \frac{E_{FS}}{2d} \left[ (N_L + 1)d_S \right. \\
& - \frac{1}{k_q} \sum_{n=1}^{(N_L+1)/2} \sin\{2k_q[n(d_F + d_S) - d_F]\} \\
& \left. - \sin[2k_q(n-1)(d_F + d_S)] \right]. \quad (6b)
\end{aligned}$$

The self-consistency condition, Eq. (3), is now transformed into

$$\begin{aligned}
\Delta(z) = & \frac{2\pi\lambda(z)}{k_F d} \sum_{p,p'} \sum_q \int d\varepsilon_{\perp} [u_{np}^{\uparrow} v_{np'}^{\downarrow} + u_{np}^{\downarrow} v_{np'}^{\uparrow}] \\
& \times \sin(k_p z) \sin(k_{p'} z) \tanh(\varepsilon_n/2T), \quad (7)
\end{aligned}$$

where  $\lambda(z) = g(z)N(0)$ , and  $N(0)$  is the DOS for one spin of the superconductor in the normal state. The quantum numbers  $n$  encompass the continuous transverse energy  $\varepsilon_{\perp}$  and the quantized longitudinal momentum index  $q$ .

The primary quantity of interest is the local density of one particle excitations in the system,  $N(z, \varepsilon)$ . Current experimental tools such as the scanning tunneling microscope (STM) have atomic scale resolution, and make this quantity experimentally accessible. Since we assume that well-defined quasiparticles exist, the tunneling current is simply expressed as a convolution of the one-particle spectral function of the STM tip with the spectral function for the ferromagnet-superconductor system.<sup>42</sup> The resultant tunneling conductance, which is proportional to the DOS, is then given as a sum of the individual contributions to the DOS from each spin channel. We have

$$N(z, \varepsilon) = N_{\uparrow}(z, \varepsilon) + N_{\downarrow}(z, \varepsilon), \quad (8)$$

where the local DOS for each spin state is given by

$$N_{\uparrow}(z, \varepsilon) = - \sum_n \{ [u_n^{\uparrow}(z)]^2 f'(\varepsilon - \varepsilon_n) + [v_n^{\uparrow}(z)]^2 f'(\varepsilon + \varepsilon_n) \}, \quad (9a)$$

$$N_{\downarrow}(z, \varepsilon) = - \sum_n \{ [u_n^{\downarrow}(z)]^2 f'(\varepsilon - \varepsilon_n) + [v_n^{\downarrow}(z)]^2 f'(\varepsilon + \varepsilon_n) \}. \quad (9b)$$

Here thermal broadening is accounted for in the term involving the derivative of the Fermi function  $f$ ,  $f'(\varepsilon) = \partial f / \partial \varepsilon$ .

We shall see below that we will also need to compare different self-consistent states. In general this is done in terms of the free energy. However, we will consider here only the low temperature limit. For  $T \rightarrow 0$ , the entropy term can be neglected, as it vanishes proportionally to  $T^2$ . In this case all we need is the ground state energy  $E_0$ . In evaluating

this quantity some care must be taken in properly including all energy shifts, even in the bulk case.<sup>43,44</sup> In the inhomogeneous case the result<sup>45</sup> can be written as

$$E_0 = \int_0^d dz \int_{-\infty}^0 \varepsilon N(z, \varepsilon) d\varepsilon + \frac{1}{g} \langle |\Delta(z)|^2 \rangle, \quad (10)$$

where the angular brackets in  $\langle |\Delta(z)|^2 \rangle$  denote the spatial average, and  $N(z, \varepsilon)$  is given in Eq. (8). One can rewrite  $E_0$  in a somewhat more standard way:

$$E_0 = - \sum_p \sum_n' \varepsilon_n [(v_{np}^{\uparrow})^2 + (v_{np}^{\downarrow})^2] + \frac{1}{g} \langle |\Delta(z)|^2 \rangle, \quad (11)$$

which in principle gives  $E_0$  in terms of the calculated excitation spectra.

### III. RESULTS

In this section we present and discuss the results that we have obtained through our numerical solution of the matrix eigensystem, Eq. (4), and the self-consistency condition Eq. (7). We will study the two cases of  $N_L = 3$  and  $N_L = 5$ , that is, *SFS* and *SFSFS* structures separately. We consider only “regular” structures in which all *S* layers have the same thickness  $d_S$ , which we will take to be a fixed value larger than  $\xi_0$ , while the *F* layers, when there is more than one, all have the same thickness,  $d_F$ , which we will vary over a certain range while keeping these layers thin enough so that we can study the periodicity in  $d_F$  of the relative stability of the  $\pi$  state. Structures with these characteristics are experimentally feasible.<sup>46,47</sup> Our characterization of these structures as regular might be questioned on the grounds that, when there are more than two *S* layers, the two at the edges do not play the same role as the others: since the central *S* layers have neighboring *F* layers on both sides, choosing their thickness to be twice that of the edge layers might be thought of as more regular. For our purpose, however, which is that of studying the relative stability of the  $\pi$  state as a function of  $d_F$  for structures of no more than five layers at low  $T$ , while keeping  $d_S > \xi_0$ , our choice is perfectly adequate. Nevertheless, for other purposes, such as studying the transition temperature of superlattices made of relatively thin<sup>27,28</sup> *S* and *F* layers as a function of layer number, the situation is quite different, and it is then more consistent to halve the thickness of the outer layers.

With the assumption that no current flows across the sample, the quantity  $\Delta(z)$  can be taken to be real, but it can in principle switch sign (0 or  $\pi$  state) in going from one *S* layer to the next. In our calculations we have studied two different values of the parameter  $I$ ,  $I = 0.5$  and  $I = 1$ . We have set the superconducting correlation length  $\xi_0$  to  $\Xi_0 \equiv k_S \xi_0 = 50$ , where  $k_S$  is the Fermi wave vector of the superconductor, and taken  $\omega \equiv \omega_D / E_{FS} = 0.1$  for the dimensionless Debye energy cutoff. It follows from previous studies<sup>40</sup> that the first of these parameters simply sets the overall length scale in the superconductor and is of little relevance whenever  $d_S$  exceeds  $\xi_0$ , as will be the case here, while the second is unimportant at low temperatures (the limit that we will consider), as it simply sets the scale for  $T_c$ . We have also

assumed that there is no oxide barrier between the layers and that the “mismatch parameter”  $\Lambda = (E_{FM}/E_{FS})$  is unity. A nonzero barrier height would in general diminish the amplitude of all the phenomena discussed here, without qualitatively altering the results. The possible influence of varying  $\Lambda$  is more complicated: this parameter<sup>40</sup> determines, together with  $I$ , the basic spatial periodicity of the problem,  $\xi_F \approx (k_\uparrow - k_\downarrow)^{-1}$ , (where  $k_\uparrow$  and  $k_\downarrow$  are, respectively, the Fermi wave vectors of the parabolic up and down spin bands in the ferromagnet), which we shall see is very important here. Furthermore, the amplitude of the oscillatory behavior found in simpler  $SF$  structures decreases<sup>40</sup> with  $\Lambda$ .

As explained in previous work (see Refs. 39 and 40), the self-consistent solution to these equations is obtained iteratively: one makes a suitable initial guess for  $\Delta(z)$ , diagonalizes the system equation (4) for that guess, and computes an iterated  $\Delta(z)$  from Eq. (7). The process is then repeated until convergence is obtained. The technicalities for the self-consistent solution of these equations were extensively discussed in previous work.<sup>40,48</sup> The diagonalization in terms of the orthonormal basis chosen must be performed for each value of  $\varepsilon_\perp$  in the appropriate range. We took here  $N_\perp = 5000$  different values of  $\varepsilon_\perp$ , except as indicated below, and the number of basis functions required for convergence was up to  $N = 1000$ . The self-consistent solution process is terminated when the relative error between consecutive iterated values of  $\Delta(z)$  nowhere exceeds  $10^{-4}$ . We have found that the number of iterations needed to achieve self-consistency can be quite large: in most cases, it exceeds 50.

Because our objective here is to discuss the possible  $\pi$  states, in starting the iteration process we make two different initial guesses: one is of the ordinary “0” state form, where the initial guess has the same sign (conventionally positive) in all the superconducting layers, and one of the  $\pi$  form, where it alternates sign from one  $S$  layer to the next. We have found that in some cases, for example, for  $SFS$  structures with small  $d_S$  (i.e.,  $d_S \lesssim \xi_0$ ), and  $d_F \lesssim \pi \xi_F$ , the self-consistent  $\Delta(z)$  typically converges to either a 0 or  $\pi$  state regardless of the initial guess, depending on  $d_F$ . A similar trend holds for the small  $d_S$  five-layer  $SFSFS$  system but over a broader  $d_F$  range. However, for the regular structures that we will focus on here, with  $d_S \gg \xi_0$ , two different self-consistent solutions are *always* obtained, one of the 0 and one of the  $\pi$  type, according to the type of initial guess. We interpret this as showing that two local minima of the free energy exist. We then have to determine the stable minimum by calculating the free energy (or rather, at low temperature, the ground state energy) of both self-consistent states, as discussed below, and comparing them.

### A. $SFS$ structure

We consider first the case of a  $SFS$  sandwich. Preliminary investigations showed that the situation of interest occurs when the magnetic layer is not too thick. This is as expected, since the overall length over which the superconducting correlations penetrate (in an oscillatory way) into the magnet is characterized by  $(k_\uparrow - k_\downarrow)^{-1}$ , which at the relatively large values of  $I$  considered here is fairly small. Thus, we have

taken in the studies presented here a thickness  $k_S d_S = 300$  for the superconducting layers, and the parameter  $k_S d_F$  meanwhile is varied in the range between 1 and 20. The choice of  $k_S d_S$  determines, through standard BCS theory relations, the value of the ratio of the superconductor Fermi energy to the bulk order parameter.

As explained above, results were obtained by iteration from two initial configurations of  $\Delta(z)$ , with the initial guesses corresponding to opposite signs for the pair potential in each of the two  $S$  layers. For the range of parameters considered here, both initial guesses led in all cases to self-consistent configurations, which were either of the 0 or of the  $\pi$  types, according to the initial guess. This is described in Fig. 2, where we show examples of the two self-consistent solutions for the pair amplitude  $F(Z)$ , as a function of the dimensionless distance  $Z \equiv k_S z$ . It is not surprising that both types of solutions are found: it is after all obvious that in the limit where  $d_F$  is sufficiently large, both solutions must exist and be degenerate. The pair amplitude  $F(z) = g\Delta(z)$  does not vanish identically in the magnetic region, but it exhibits the well-known oscillations. In the superconductor, it rises in absolute value towards the bulk result, away from the  $S/F$  interfaces. Results are shown for  $I = 0.5$  at three values of  $k_S d_F$ . We can see that in certain cases, depending on the thickness of the  $F$  layer,  $F(z)$  in the superconductor [and hence  $\Delta(z)$ ] is larger, in absolute value, for the 0 than for the  $\pi$  state (see top panel), while in some other cases (middle panel) the opposite occurs, and for yet some other  $d_F$  values (see the bottom panel) there is no observable difference. Intuitively, this happens because of the different way, depending on  $k_S d_F$ , in which the pair amplitude in the two superconductor regions must adjust itself to the oscillations in the magnet. That the oscillatory behavior of the pair amplitude in the  $F$  layer is clearly different for the 0 and  $\pi$  solutions can be seen by careful examination of the portion of the plots that lies in the  $F$  region.

To find out the most stable configuration, one must compute the difference in the ground state energies, or equivalently the condensation energies, of the 0 and  $\pi$  states. This can be done in principle by using Eq. (11). In practice this is computationally very difficult: the value of  $E_0$  for each state must be computed separately from its own spectrum (which can consist of up to  $10^6$  eigenstates), and the results subtracted. Since each  $E_0$  includes the normal state energy, which is many orders of magnitude larger than the condensation energy sought, this requires extreme numerical accuracy. The problem is exacerbated because the “logarithmic” last term on the right-hand side of Eq. (11) is in itself much larger than the condensation energy (and the latter is itself considerably larger, as we shall see below, than the condensation energy *difference* between the two states), and must be exactly canceled by a portion of the first term. This is a well-known problem even in the bulk case, where great care has to be taken<sup>43</sup> to make the delicate cancellation analytically explicit. We have found it technically impractical to numerically compute  $E_0$  from Eq. (11) for all cases considered<sup>49</sup> with the required precision. However, by using increased values of  $N_\perp$  and  $N$  in a few selected cases we have been able to verify that the ground state *condensation*

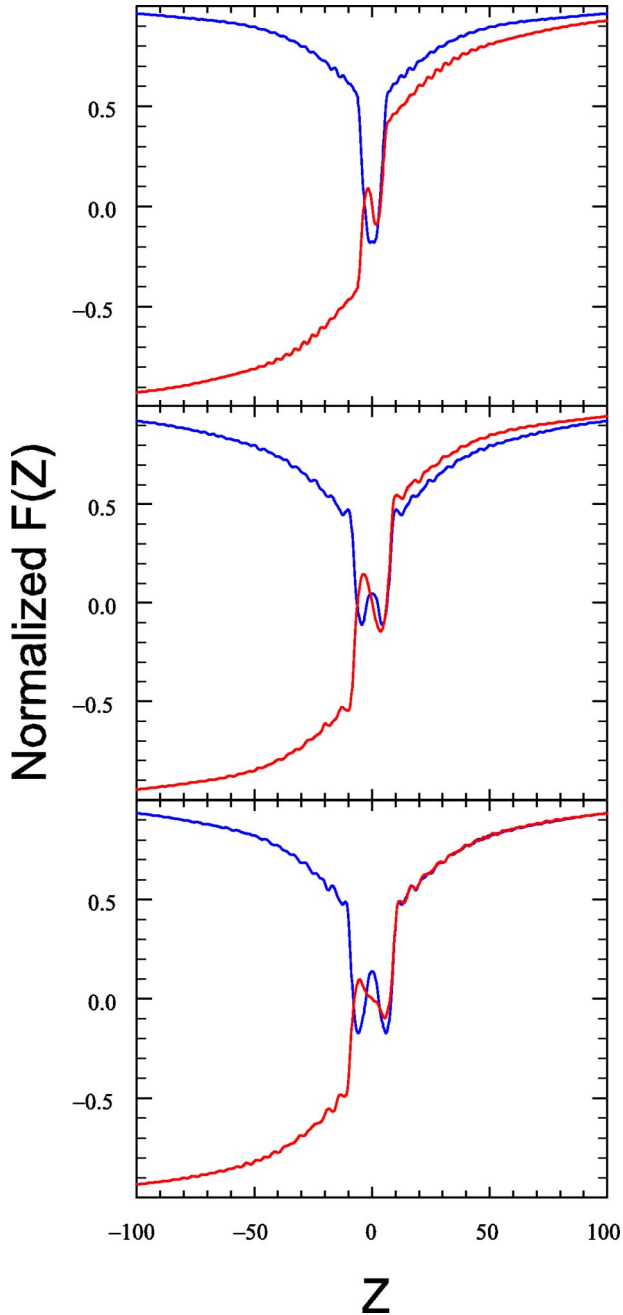


FIG. 2. (Color online) Results for the pair amplitude  $F(Z)$ , normalized to the bulk superconductor value, as a function of  $Z \equiv k_S z$ , in a  $SFS$  structure. The dimensionless thickness of the  $S$  portions is  $k_S d_S = 300$ , while the corresponding values of the dimensionless thickness of the intervening  $F$  layer are (from top to bottom)  $k_S d_F = 10, 16, 19$ . The blue (darker) lines represent self-consistent solutions of the 0 type, and the red (lighter) lines alternative self consistent solutions of the  $\pi$  type. The value of  $I$  is 0.5, and the dimensionless superconducting correlation length is  $k_S \xi_0 = 50$ .

energy (that is, after subtracting the normal ground state energy  $E_{0n}$  calculated for the same geometry and parameter values except for setting  $g=0$ ) for either the 0 or  $\pi$  states is, for the cases considered here where  $d_F$  is small and  $d_S \gg \xi_0$ , approximately given by

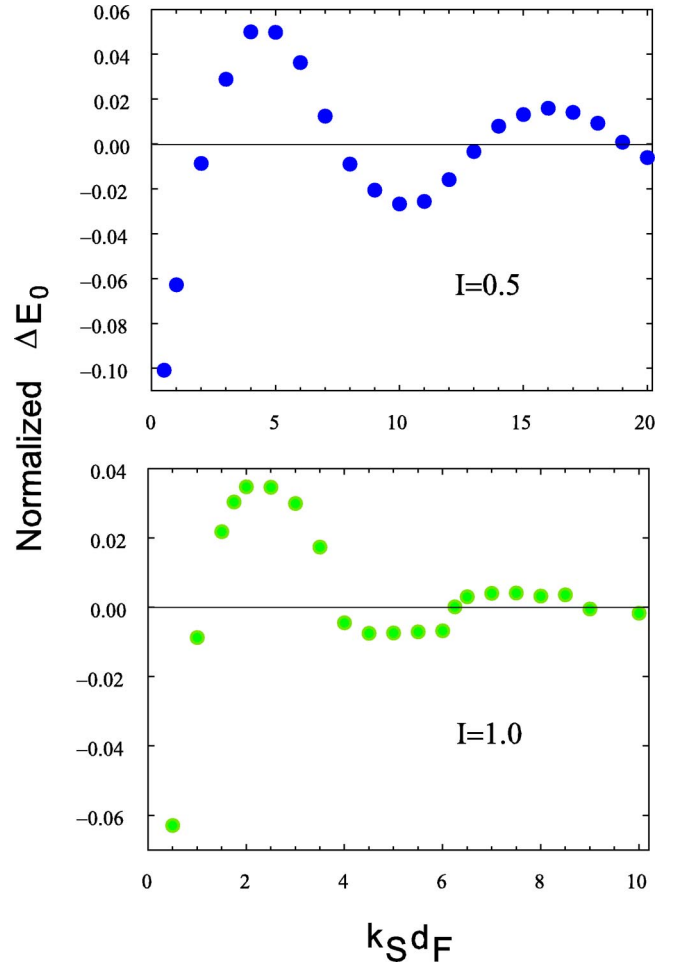


FIG. 3. (Color online) The difference in condensation energies,  $\Delta E_0$ , between the 0 and  $\pi$  states for a  $SFS$  sandwich in the low-temperature limit, normalized to  $2N(0)\Delta_0^2$ , calculated as explained in the text. The results are plotted as a function of the dimensionless thickness  $k_S d_F$  of the ferromagnetic layer, for two values of  $I$ . At small  $d_F$  the zero state is favored. The periodicity of the results is determined by  $(k_\uparrow - k_\downarrow)^{-1}$ , as expected.

$$E_0 - E_{0n} \approx -\alpha N(0) \langle |\Delta|^2 \rangle. \quad (12)$$

This result is *a posteriori* not surprising at all in the limit of large  $d_S$  and small  $d_F$ , as it is quite similar to what is found<sup>50</sup> analytically for the bulk: in that case  $\alpha$  is exactly 0.5 and the spatial average is of course replaced by the uniform bulk value. In our case we find the coefficient  $\alpha < 0.5$  within our numerical uncertainty. The right-hand side of Eq. (12) is of course very easy to compute. Thus, we have adopted a procedure based on Eq. (12) to compare condensation energies for the two competing states.

The results are shown in Fig. 3. The quantity plotted there is the difference between the values of  $\langle |\Delta|^2 \rangle$  for the 0 and  $\pi$  states normalized to  $2N(0)\Delta_0^2$ , where  $\Delta_0$  is the bulk gap. This normalization corresponds to twice the bulk value limit of the condensation energy. This is then a dimensionless measure of the condensation (or equivalently, ground state) energy difference between the self consistent 0 and  $\pi$  configurations [see Eq. (12)]. This normalized energy difference

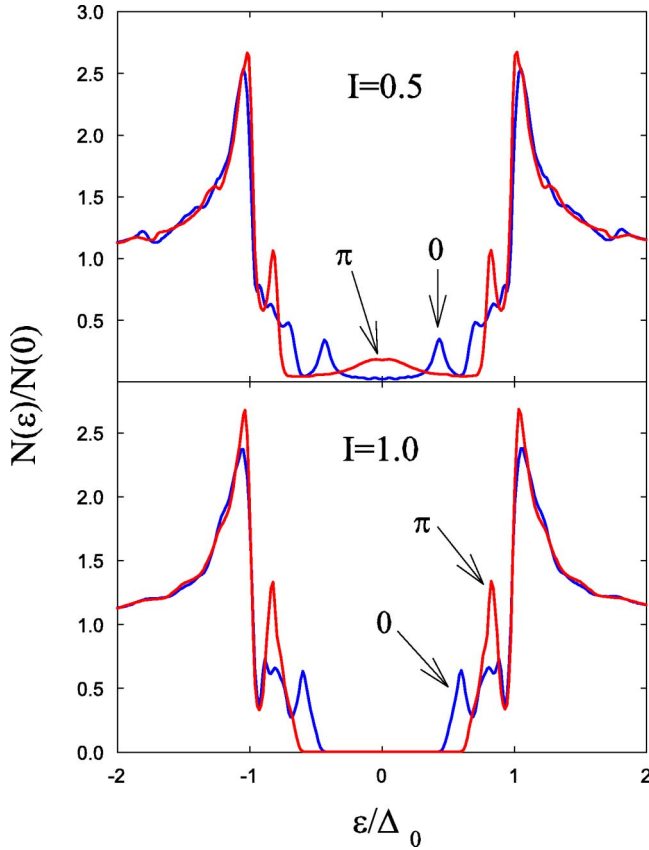


FIG. 4. (Color online) Density of states (DOS) results for *SFS* structures. The quantity plotted is the local DOS integrated over one *S* layer, normalized to  $N(0)$ . The energy is normalized to the bulk gap  $\Delta_0$ . The top panel shows results at  $k_S d_F = 5$ , where the stable state (see Fig. 3) is of the  $\pi$  type (red curve, labeled as  $\pi$ ), and at  $k_S d_F = 10$ , where the 0 state is more stable (blue solid curve, labeled 0). In the bottom panel,  $I = 1$  and, consistent with the doubling of  $I$ , the thicknesses displayed are halved to  $k_S d_F = 2.5$  ( $\pi$  case) and  $k_S d_F = 5$  (zero case). See text for discussion.

is plotted as a function of the dimensionless thickness  $k_S d_F$  of the intermediate *F* layer, which is sandwiched between thick ( $k_S d_S = 300$ ) *S* layers. We see that the difference in energies is, as one would expect, only a small fraction (about one-tenth at the most) of the bulk condensation energy. We also see that it is an oscillatory function of  $k_S d_F$ . Comparison of the top and bottom panels (which correspond to  $I = 0.5$  and  $I = 1$  respectively) shows that the rough periodicity of these results is approximately given by  $(k_\uparrow - k_\downarrow)^{-1}$ , and it is in fact very similar<sup>40</sup> quantitatively to the oscillatory behavior of the pair amplitude  $F(z)$  in a thick magnetic layer. At small  $k_S d_F$ , the 0 state is obviously very favored, as one would expect, while in the limit of large  $k_S d_F$  the energy difference is of course zero, reflecting the degeneracy of the two states. The influence of the parameter  $I$  is quite dramatic: in the half metallic case (lower panel) the first peak favoring the  $\pi$  state is more prominent and the 0 state is generally speaking less favorable than that for the intermediate value of  $I$  shown in the top panel.

We turn now to the density of states (DOS) for this geometry. Typical results are exhibited in Fig. 4, where we

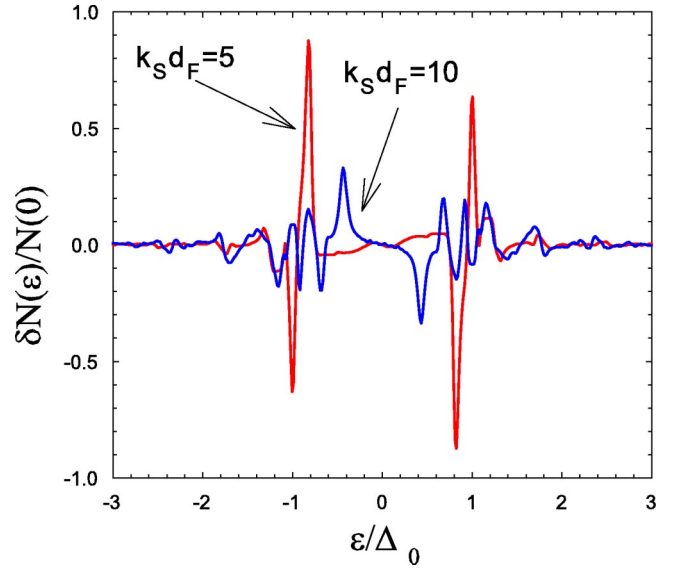


FIG. 5. (Color online) Differential density of states (DOS) between up and down spin states for *SFS* structures. The quantity plotted is that defined in Eq. (13), integrated over one *S* layer, and normalized to  $N(0)$ . Results are shown for  $I = 0.5$  at  $k_S d_F = 5$ , where the stable state (see Fig. 3) is of the  $\pi$  type (red curve) and at  $k_S d_F = 10$ , where the 0 state is more stable (blue solid curve).

show the DOS, integrated over the superconducting region of thickness  $k_S d_S = 300$ , as a function of the energy, normalized to the bulk gap  $\Delta_0$ . Results are shown for two values of  $I$  (top and bottom panels) and, for each value of  $I$ , at two values of  $k_S d_F$ , one corresponding to the case where the equilibrium state is of 0 state type, and the other corresponding to the opposite situation. One can see that for  $I = 0.5$  there are states in the gap, and that these states are more prominent in the  $\pi$  case where there is a zero energy small peak. At  $I = 1$  the DOS results are also different: although for both of the cases shown there is a gap in the spectrum, the location of the peaks near the gap edge is not the same for the 0 and  $\pi$  states, with the first peaks being more prominent and at higher energies in the latter case. Thus, there are genuine differences between the DOS of 0 and  $\pi$  states, which may be experimentally observable.

It is also of interest to show the difference between the local DOS for up and down states, as defined by

$$\delta N(z, \varepsilon) \equiv N_\uparrow(z, \varepsilon) - N_\downarrow(z, \varepsilon). \quad (13)$$

This is done in Fig. 5, where results are shown for the two cases corresponding to those also displayed in the top panel of Fig. 4. The differential DOS shown is integrated over the thickness of one *S* layer, and normalized to the total normal bulk DOS value. Because of the finite value of  $I$ , the results are not symmetric around zero energy. One can see that the energy structure at the gap edge is appreciably more prominent for the thickness value that corresponds to an equilibrium  $\pi$  state, while for the 0 state the structure is broader and more diffused.

An alternative way of illustrating the magnetic polarization effects, which has also the advantage of providing local

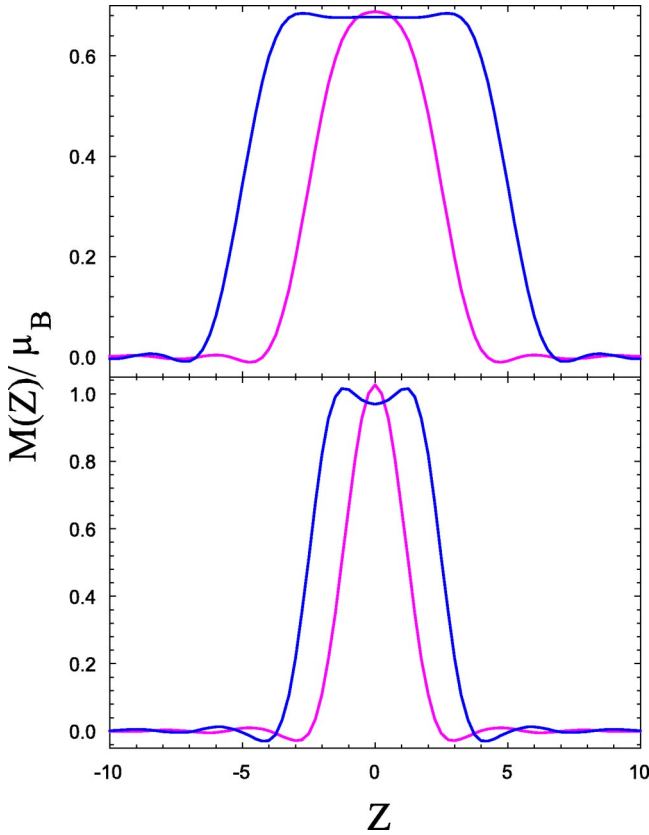


FIG. 6. (Color online) Normalized local magnetic moment as defined in the text and Eq. (15). Results in the top and bottom panels correspond to the same values of  $I$  and thickness as in the corresponding panels of Fig. 4. Thus the top panel is for  $I=0.5$  and  $k_S d_F=5,10$ , while the bottom panel is for  $I=1$  and  $k_S d_F=2.5,5$ .

information, is through the use of the local magnetic moment  $m(z)$ . This quantity is easily obtained by integration of the local DOS results. One has

$$m(z) = \mu_B \int d\varepsilon \delta N(z, \varepsilon) f(\varepsilon), \quad (14)$$

where  $\mu_B$  is the Bohr magneton and the integral extends over the occupied states in the band. This can be cast in a more convenient form as

$$m(z) = \mu_B [\langle n_\uparrow(z) \rangle - \langle n_\downarrow(z) \rangle], \quad (15)$$

where  $\langle n_\sigma(z) \rangle$  is the average number density for each spin subband, and is written in terms of the quasiparticle amplitudes as

$$\langle n_\sigma(z) \rangle = \sum_n \{ [u_n^\sigma(z)]^2 f(\epsilon_n) + [v_n^\sigma(z)]^2 [1 - f(\epsilon_n)] \},$$

$$\sigma = \uparrow, \downarrow. \quad (16)$$

It is more instructive to plot  $m(z)$  normalized to the corresponding integral of  $N_\uparrow(z, \varepsilon) + N_\downarrow(z, \varepsilon)$ . We denote this normalized quantity by  $M(z)$  and we plot it, in units of the Bohr magneton, in Fig. 6. The two panels there correspond to values of  $I$  and  $k_S d_F$  as in the corresponding top and bottom

panels of Fig. 4. We see in this figure that for relatively small  $k_S d_F$ , the quantity plotted rises up sharply from the  $F/S$  interface and then has a slow modulation as it approaches its bulk value in the  $F$  layer. The magnetization does not vanish identically inside the superconductor: its behavior there consists of strongly damped oscillations, with an overall characteristic spatial decay on the order of a few Fermi wavelengths. The effect does not seem to depend strongly on whether one is dealing with 0 or  $\pi$  states.

The self-consistent results displayed can also be interpreted as representing an effective, local value of  $I(z)$ , through the relation  $M(z) = \mu_B \{ [1 + I(z)]^{3/2} - [1 - I(z)]^{3/2} \} / \{ [1 + I(z)]^{3/2} + [1 - I(z)]^{3/2} \}$ . The quantity  $I(z)$  is then the magnetic counterpart of the self-consistent  $F(z)$ , measuring directly the magnetic part of the proximity effect, that is, the leakage of magnetic correlations into the superconductor.

### B. SFSFS structure

In this section we consider the case of more complicated, five-layer structures. These are realizable experimentally<sup>31</sup> and therefore of considerable interest. As in the three-layer case, we will study the situation where the three superconducting layers are relatively thick, taking again  $k_S d_S = 300$ , and as stated above, the  $F$  layers are thin enough so that  $F/S$  proximity effects cannot be neglected.

We begin by considering (see Fig. 7) the pair amplitude  $F(z)$ . This figure is in every way analogous to Fig. 2, except for the insets, where we display in more detail the behavior of  $F(z)$  in one of the ferromagnetic layers. Results for solutions of both the 0 and the  $\pi$  type are shown. Both are obtained self-consistently, the first by starting from an initial guess in which the sign of the order parameter in the three  $S$  layers is always the same, and the second by starting with a guess in which the order parameter in the middle  $S$  layer is opposite to that in the other two layers. Self-consistent solutions are always reached, upon iteration, for large  $d_S$  and  $d_F$  in the ranges shown, in either case. We observe the expected depletion of  $F(z)$  near the  $F/S$  interfaces, and the subsequent approach toward its bulk value over the length scale  $\xi_0$ , with the maximum  $\Delta(z)$  in the central  $S$  layer only very slightly reduced from the bulk  $\Delta_0$ . We also see in the main panels that depending on the value of  $k_S d_F$ , the absolute value of  $F(z)$  in the superconductors varies periodically between being larger in the 0 state to being larger in the  $\pi$  state, as was the case for three-layer structures. The insets illustrate more clearly how the existence of the two states relates to the oscillations of  $F(z)$  in the ferromagnetic region, which are very different in each case.

As in the three-layer case, therefore, we find that there are two local minima of the free energy, corresponding to the 0 and  $\pi$  alternatives. Again, the absolute minimum, at low temperature, must be found by comparing the two condensation energies. This we do in the same way as for the three-layer case [see Eq. (12) and associated discussion]. The results are shown in Fig. 8, which should be compared with Fig. 3. The two figures are remarkably similar. In both cases the behavior is oscillatory, with the same approximate spatial



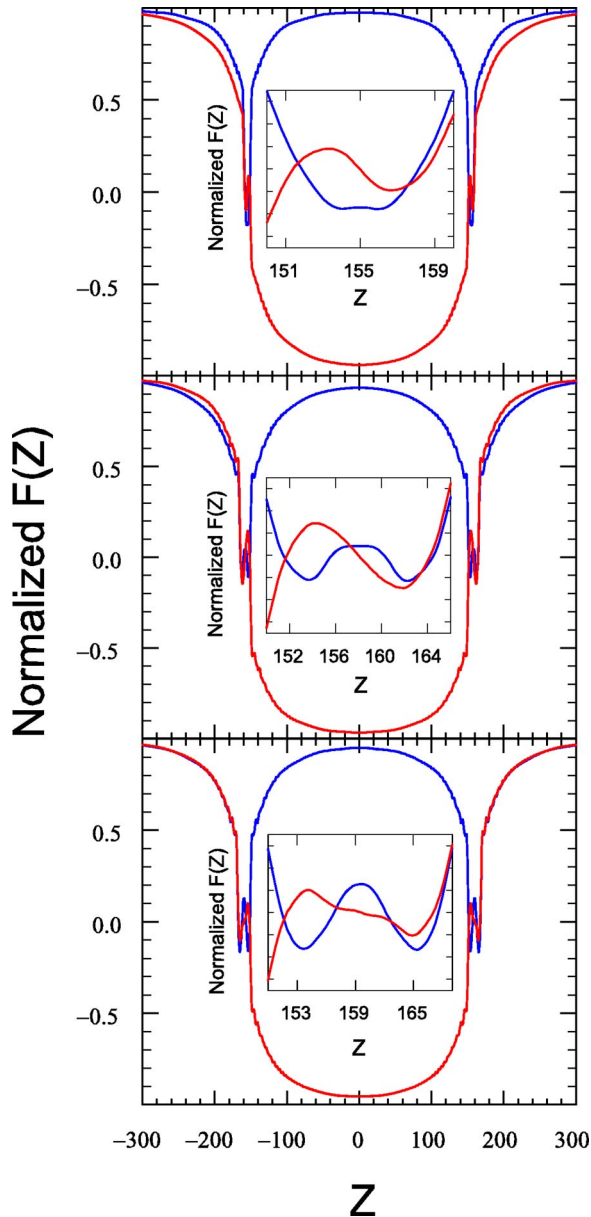


FIG. 7. (Color online) Results for the pair amplitude  $F(Z)$ , normalized to the bulk superconductor value, as a function of  $Z \equiv k_S z$ , in an  $SF/SF/SF/SF/SF$  structure, for  $I=0.5$ . The dimensionless thickness of the  $S$  portions is  $k_S d_S = 300$ , and the corresponding values of the dimensionless thickness of the intervening  $F$  layer are (from top to bottom)  $k_S d_F = 10, 16, 19$ . The blue (darker) lines represent self-consistent solutions of the zero type, and the red (lighter) lines of the  $\pi$  type. The insets are a magnification of one of the  $F$  regions. The vertical axis in the insets varies between  $\pm 0.35$  in dimensionless units.

periodicity related to that of the pair amplitude oscillations. Again, the obvious results that the 0 state is favored at small  $k_S d_F$  and that the two states are degenerate for large  $k_S d_F$  are recovered. The three- and five-layer plots are not identical, however: in the latter case we find that the overall scale of the phenomenon is nearly a factor of 2 higher, as one can see by comparing the vertical axes. This difference may be due in part to the enlarged proximity effect in the the middle  $S$

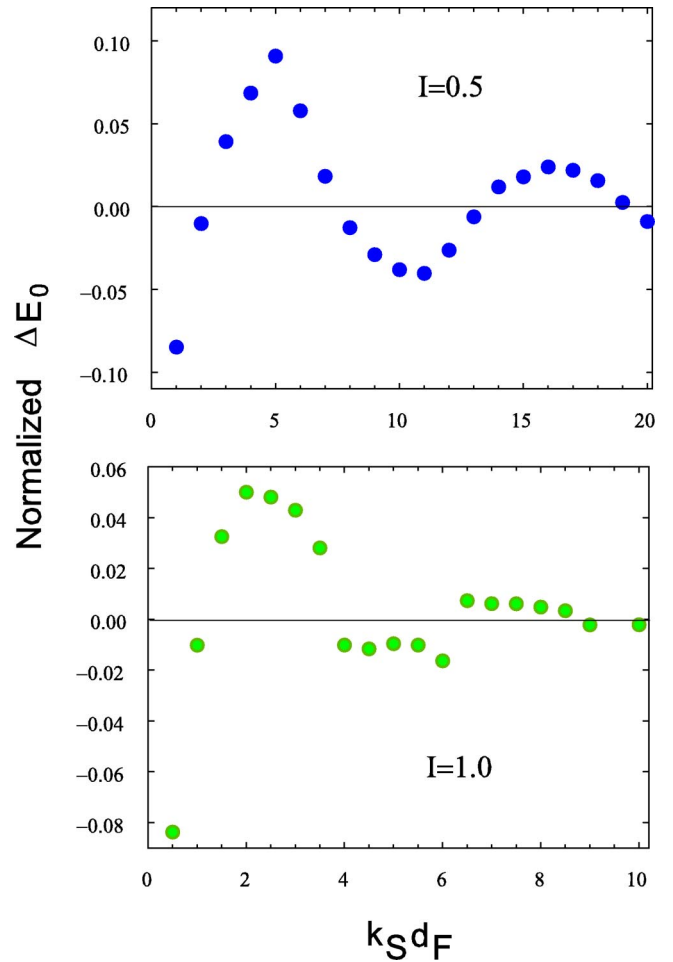


FIG. 8. (Color online) Difference in condensation energies,  $\Delta E_0$ , between the 0 and  $\pi$  states for a five-layer  $SF/SF/SF/SF/SF$  system, calculated as explained in the text, and normalized to  $2N(0)\Delta_0^2$ , as in Fig. 3. This quantity is plotted as a function of the thickness  $k_S d_F$  of each ferromagnetic layer. Results for two values of  $I$  are shown.

layer, which has a ferromagnet on each side. The first peak favoring the  $\pi$  state is higher and sharper for five layers. Although the effect of increasing the layer number is not as dramatic as that of increasing  $I$ , one can nevertheless assert from the trend that the oscillatory behavior with  $d_F$  would not only persist but would be even more prominent if the number of layers were further increased, as in superlattices.

A few selected DOS results for this  $SF/SF/SF$  geometry are shown in Fig. 9, which should be viewed in comparison with the analogous Fig. 4 for the  $SFS$  structure. The quantity plotted is averaged over one of the two outside  $S$  layers, and all parameters are chosen to be the same as in Fig. 4. The similarity between the two figures is at first sight very remarkable, although a second look shows that the structure of the subgap peaks is far from being the same, particularly for the 0 state case, where additional shoulders appear at  $I=1$ . One concludes again that many features, including the 0 energy peak in the stable  $\pi$  state of the top panel, are robust with respect to increasing the number of layers, and very likely to persist, and even be more obvious, in larger regular structures.

The differential DOS between up and down states for this

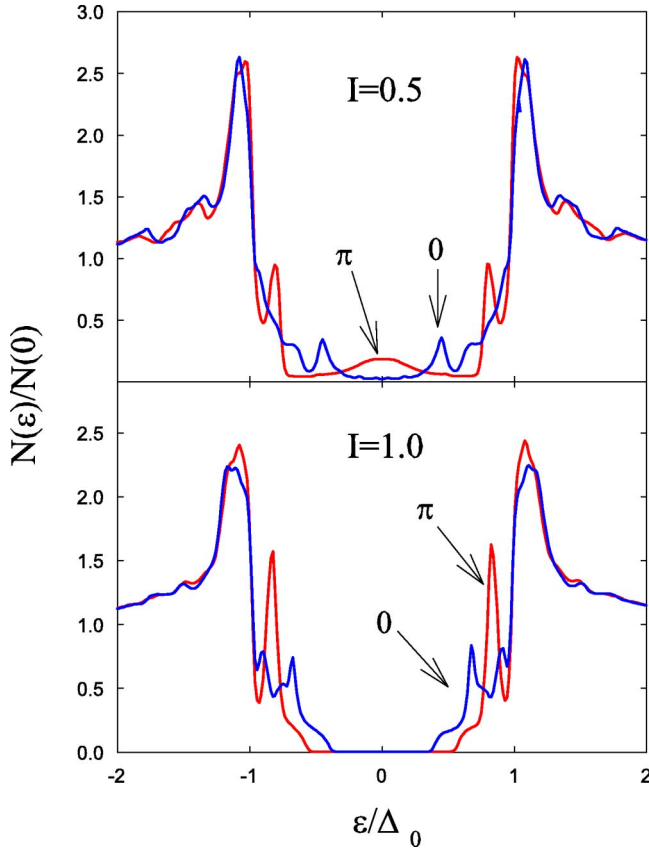


FIG. 9. (Color online) Density of states (DOS) results for SF/SFS structures. The local DOS integrated over one of the external S layers, normalized to  $N(0)$ , is plotted vs the energy normalized to the bulk gap  $\Delta_0$ . The top panel shows results at  $k_S d_F = 5$ , where the stable state (see Fig. 8) is of the  $\pi$  type (red curve, labeled as  $\pi$ ) and at  $k_S d_F = 10$ , where the 0 state is more stable (blue solid curve, labeled 0). In the bottom panel,  $I = 1$  and the thicknesses are  $k_S d_F = 2.5$  ( $\pi$  case) and  $k_S d_F = 5$  (0 case).

geometry exhibits a behavior sufficiently similar to that displayed in Fig. 5 for the SFS case that there is no need to display it in a separate figure here. On the other hand, it is worthwhile to illustrate an example of the normalized local magnetic moment  $M(z)$ . This is done on Fig. 10, where this quantity, as defined in Eq. (14) is plotted with the same normalization and parameter values as in the top panel of Fig. 6. The behavior for the two geometries is certainly similar, but one again sees that the magnetic penetration effects become slightly more prominent as the number of layers increases from three to five. This is another indication that such effects are very likely to be easier to observe in structures involving a larger number of layers.

#### IV. CONCLUSIONS

We have rigorously investigated the proximity effects that occur in clean multilayered F/S structures of the SFS and SF/SFS types. We used a microscopic wave function approach that does not coarse grain the microscopic variables over length scales of order  $\lambda_F$ , and thus accounts for atomic-scale effects. The space dependence of the pair amplitude

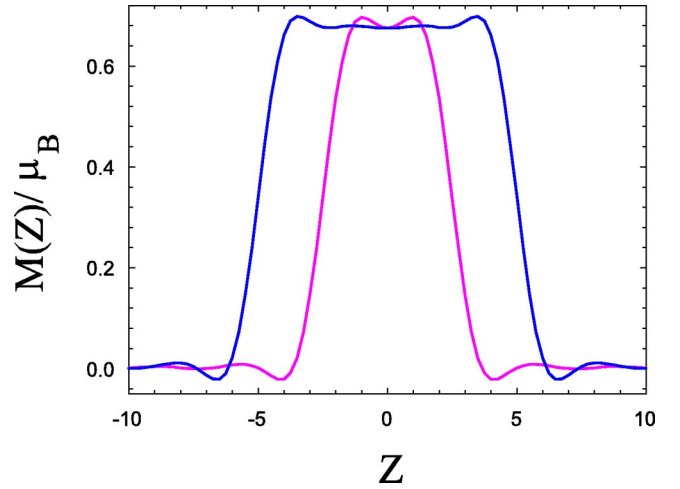


FIG. 10. (Color online) Normalized local magnetic moment for an SF/SFS structure, as defined in the text and Eq. (14). Results are for  $I = 0.5$  and  $k_S d_F = 5, 10$ .

$F(z)$  was obtained self-consistently by using an efficient numerical algorithm. From the calculated eigenstates, we were then able to obtain the experimentally relevant local magnetic moment and the local density of states.

We have demonstrated that for all the cases considered, where the thickness  $d_S$  of the superconducting layers is much greater than  $\xi_0$  and that of the ferromagnetic regions is relatively small, two local minima of the ground state energy exist, yielding self-consistent states of the 0 and  $\pi$  types. Through a careful analysis of the pair amplitude and excitation spectrum, we have calculated which of these two states is the actual ground state, with the lowest energy. The results show that the difference in condensation energies between the 0 and  $\pi$  states exhibits damped oscillations as a function of ferromagnet width, with the characteristic exchange-field-dependent spatial period being given approximately as  $2\pi(k_\uparrow - k_\downarrow)^{-1}$ , the same quantity that characterizes the oscillations of  $F(z)$  in bilayers. The local DOS exhibits strikingly different behavior for two exchange fields that differed by a factor of 2. For  $I = 0.5$ , the subgap DOS shows a gapless structure, with features that depend strongly on whether the ferromagnet width corresponds to the 0 or  $\pi$  state. The half-metallic case ( $I = 1.0$ ) is, on the other hand, gapless in the range of  $d_F$  considered, and the modified excitation spectrum reveals itself through the differing peaks in the DOS. To illustrate the leakage of magnetism into the superconductor, the differential DOS between the spin up and spin down states was presented for a SFS junction. The most prominent spin splitting was seen for the  $\pi$  junction at energies  $\epsilon/\Delta_0 \approx 1$ . We believe that this represents an experimentally important signature for the  $\pi$  state. We have also calculated the local magnetic moment for both the three and five layer cases, to give further insight into magnetic polarization effects. Although we found the results to be relatively insensitive to a 0 or  $\pi$  state configuration, we were able to extract an effective local value of  $I(z)$  in both the F and S layers.

The calculations and method used in this paper, although sufficiently general to include in the future more complicated effects (e.g., finite temperature, other pairing states, spin-flip

scattering, and impurities), were taken within the ballistic limit. This limit is appropriate for ferromagnet layers whose width is less than the mean free path, and this is consistent with our calculations, where we have taken  $k_S d_F \leq 20$ . The inclusion of interfacial scattering would likely have the effect of diminishing the proximity effect, without qualitatively altering the characteristic results. For bulk impurity scattering, the effective  $\xi_F$  would involve not just  $l$  but also the diffusion length. It is the goal of future work to address these

topics, and also others, including heterostructures comprised of a single superconductor sandwiched between two ferromagnets with arbitrary relative magnetization,  $F/S$  multilayers with a greater number of layers, and smaller superconductor widths, where geometrical and atomic-scale effects are likely to be more prevalent.

#### ACKNOWLEDGMENT

We thank Igor Žutić for many useful discussions.

\*Email: klaus.halterman@navy.mil

†Email: otvalls@umn.edu

- <sup>1</sup>G. Blatter, V.B. Geshkenbein, and L.B. Ioffe, Phys. Rev. B **63**, 174511 (2001).
- <sup>2</sup>L.R. Tagirov, Phys. Rev. Lett. **83**, 2058 (1999).
- <sup>3</sup>A.I. Buzdin, A.V. Vedyayev, and N.V. Ryzhanova, Europhys. Lett. **48**, 686 (1999).
- <sup>4</sup>B. Nadgorny and I.I. Mazin, Appl. Phys. Lett. **80**, 3973 (2002).
- <sup>5</sup>S. Oh, D. Youm, and M.R. Beasley, Appl. Phys. Lett. **71**, 2376 (1997).
- <sup>6</sup>A. F. Andreev, Zh. Éksp. Teor. Fiz. **46**, 1823 (1964) [Sov. Phys. JETP **19**, 1228 (1964)].
- <sup>7</sup>P. Fulde and A. Ferrell, Phys. Rev. **135**, A550 (1964).
- <sup>8</sup>A. Larkin and Y. Ovchinnikov, Zh. Éksp. Teor. Fiz. **47**, 1136 (1964) [Sov. Phys. JETP **20**, 762 (1965)].
- <sup>9</sup>N.M. Chtchelkatchev, W. Belzig, Y.V. Nazarov, and C. Bruder, Pis'ma Zh. Éksp. Teor. Fiz. **74**, 101 (2001) [JETP Lett. **74**, 96 (2001)].
- <sup>10</sup>A.Y. Zyuzin, B. Spivak, and M. Hruska, Europhys. Lett. **62**, 97 (2003).
- <sup>11</sup>A. Zenchuk and E. Goldobin, nlin.PS/0304053 (unpublished).
- <sup>12</sup>A.F. Volkov, F.S. Bergeret, and K.B. Efetov, Phys. Rev. Lett. **90**, 117006 (2003).
- <sup>13</sup>M. Krawiec, B.L. Gyorffy, and J.F. Annett, Phys. Rev. B **66**, 172505 (2002).
- <sup>14</sup>Z. Radović, L. D-Grujic, and B. Vujicic, Phys. Rev. B **63**, 214512 (2001).
- <sup>15</sup>A.I. Buzdin and M.Y. Kuprianov, Pis'ma Zh. Éksp. Teor. Fiz. **53**, 308 (1991) [JETP Lett. **53**, 321 (1991)].
- <sup>16</sup>A. Buzdin and I. Baladie, Phys. Rev. B **67**, 184519 (2003).
- <sup>17</sup>E.A. Demler, G.B. Arnold, and M.R. Beasley, Phys. Rev. B **55**, 15174 (1997).
- <sup>18</sup>F.S. Bergeret, A.F. Volkov, and K.B. Efetov, Phys. Rev. B **64**, 134506 (2001).
- <sup>19</sup>A.V. Andreev, A.I. Buzdin, and R.M. Osgood III, Phys. Rev. B **43**, 10124 (1991).
- <sup>20</sup>V. Prokic, A.I. Buzdin, and L. D-Grujic, Phys. Rev. B **59**, 587 (1999).
- <sup>21</sup>F.S. Bergeret, A.F. Volkov, and K.B. Efetov, Phys. Rev. Lett. **86**, 3140 (2001).
- <sup>22</sup>V.N. Krivoruchko and E.A. Koshina, Phys. Rev. B **64**, 172511 (2001).
- <sup>23</sup>V.N. Krivoruchko and R.V. Petryuk, Phys. Rev. B **66**, 134520 (2002).
- <sup>24</sup>Y.S. Barash, I.V. Bobkova, and T. Kopp, Phys. Rev. B **66**, 140503(R) (2002).
- <sup>25</sup>Z. Radović, N. Flytzanis, Phys. Rev. B **68**, 054508 (2003).

- <sup>26</sup>F.S. Bergeret, A.F. Volkov, and K.D. Efetov, Phys. Rev. Lett. **90**, 117006 (2003).
- <sup>27</sup>M.G. Khusainov and Y.N. Proshin, Phys. Rev. B **56**, 14283 (1997).
- <sup>28</sup>Y.N. Proshin, Y.A. Izyumov, and M.G. Khusainov, Phys. Rev. B **64**, 064522 (2001).
- <sup>29</sup>For an early discussion of  $F/S$  effects, see the article by G. Deutscher and P.G. de Gennes, in *Superconductivity*, edited by R.D. Parks (Dekker, New York, 1969), p. 1005.
- <sup>30</sup>A.I. Buzdin, L.N. Bulaevskii, and S.V. Panyukov, Pis'ma Zh. Éksp. Teor. Fiz. **35**, 147 (1982) [JETP Lett. **35**, 178 (1982)].
- <sup>31</sup>J.S. Jiang, D. Davidovic, D.H. Reich, and C.L. Chien, Phys. Rev. Lett. **74**, 314 (1995).
- <sup>32</sup>V.V. Ryazanov, V.A. Oboznov, A.Y. Rusanov, A.V. Veretennikov, A.A. Golubov, and J. Aarts, Phys. Rev. Lett. **86**, 2427 (2001).
- <sup>33</sup>T. Kontos, M. Aprili, J. Lesueur, F. Genet, B. Stephanidis, and R. Boursier, Phys. Rev. Lett. **89**, 137007 (2002).
- <sup>34</sup>W. Guichard, M. Aprili, O. Bourgeois, T. Kontos, J. Lesueur, and P. Gandit, Phys. Rev. Lett. **90**, 167001 (2003).
- <sup>35</sup>T. Kontos, M. Aprili, J. Lesueur, and X. Grison, Phys. Rev. Lett. **86**, 304 (2001).
- <sup>36</sup>G. Eilenberger, Z. Phys. **214**, 195 (1968).
- <sup>37</sup>K.D. Usadel, Phys. Rev. Lett. **25**, 507 (1970).
- <sup>38</sup>M. Ozana and A. Shelankov, J. Low Temp. Phys. **124**, 223 (2001); M. Ozana, A. Shelankov, and J. Tobiska, Phys. Rev. B **66**, 054508 (2002).
- <sup>39</sup>K. Halterman and O.T. Valls, Phys. Rev. B **65**, 014509 (2002).
- <sup>40</sup>K. Halterman and O.T. Valls, Phys. Rev. B **66**, 224516 (2002).
- <sup>41</sup>P.G. de Gennes, *Superconductivity of Metals and Alloys* (Addison-Wesley, Reading, MA, 1989).
- <sup>42</sup>See, e.g., F. Gygi and M. Schluter, Phys. Rev. B **41**, 822 (1990).
- <sup>43</sup>M. Tinkham, *Introduction to Superconductivity* (Krieger, Malabar, FL, 1975).
- <sup>44</sup>A.L. Fetter and J.D. Walecka, *Quantum Theory of Many-Particle Systems* (McGraw-Hill, New York, 1971).
- <sup>45</sup>I. Kosztin, Š. Kos, M. Stone, and A.J. Leggett, Phys. Rev. B **58**, 9365 (1998).
- <sup>46</sup>I.A. Garifullin, D.A. Tikhonov, N.N. Garif'yanov, L. Lazar, Yu.V. Goryunov, S.Ya. Khlebnikov, L.R. Tagirov, K. Westerholt, and H. Zabel, Phys. Rev. B **66**, 020505 (2002).
- <sup>47</sup>P. Korevaar, Y. Suzuki, R. Coehoorn, and J. Aarts, Phys. Rev. B **49**, 441 (1994).
- <sup>48</sup>K. Halterman, Ph.D. dissertation, University of Minnesota, 2002.
- <sup>49</sup>Alternative numerical methods, e.g., using infinite Fredholm determinants have been proposed (see Ref. 45 for a survey), but the precision problems remain.
- <sup>50</sup>See among many others, Ref. 43, p. 29.